

Supplementary Information

Uncovering the multifaceted roles of nitrogen defects in graphitic carbon nitride for selective photocatalytic carbon dioxide reduction: A density functional theory study

Jie-Yinn Tang,^a Chen-Chen Er,^a Lling-Lling Tan,^a Yi-Hao Chew,^a Abdul Rahman Mohamed^b and Siang-Piao Chai^{*a}

^a*Multidisciplinary Platform of Advanced Engineering, Chemical Engineering Discipline, School of Engineering, Monash University, Jalan Lagoon Selatan, Bandar Sunway, 47500 Subang Jaya, Selangor, Malaysia.*

^b*Low Carbon Economy (LCE) Group, School of Chemical Engineering, Universiti Sains Malaysia, Engineering Campus, Seri Ampangan, 14300 Nibong Tebal, Pulau Pinang, Malaysia.*

*Correspondence to: chai.siang.piao@monash.edu

Contents	Pages
Formation Energy of Defects	S1
Spatial Distribution of HOMO-LUMO	S2
CO ₂ Adsorption Simulation Details	S3
Gibbs Free Energy Change	S7

1. FORMATION ENERGY OF DEFECTS

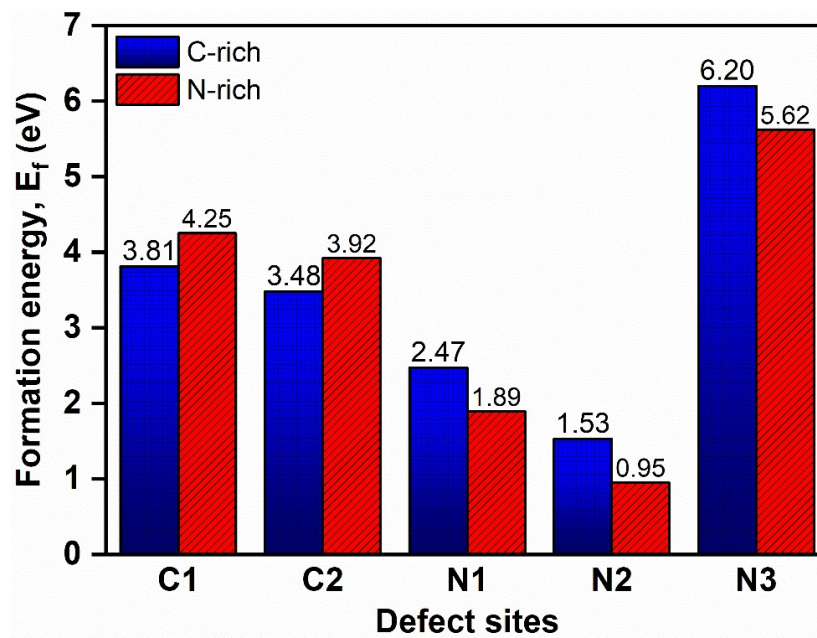


Fig. S1 Formation energy, E_f of defects in $g\text{-C}_3\text{N}_4$ at five potential sites under C-rich and N-rich conditions.

2. SPATIAL DISTRIBUTION OF HOMO-LUMO

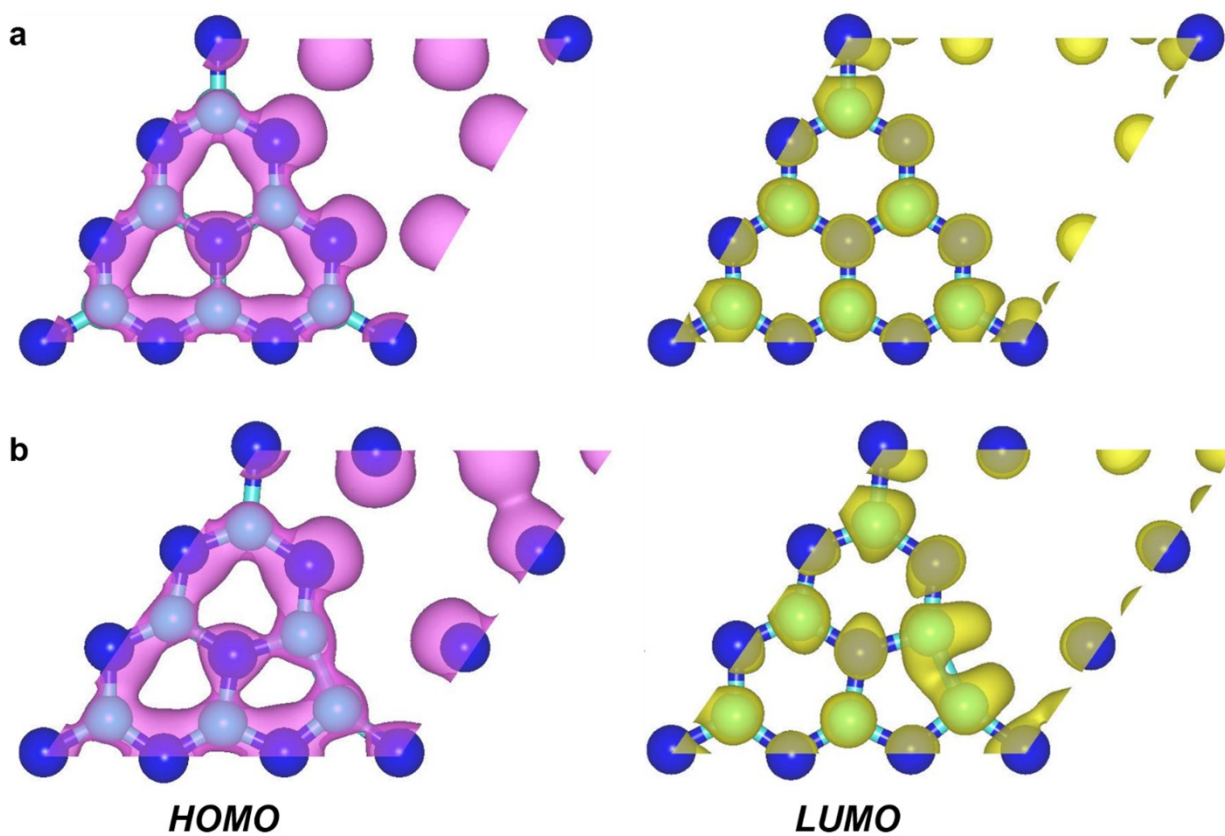


Fig. S2 Spatial distribution of the highest occupied molecular orbital (HOMO) and lowest unoccupied molecular orbital (LUMO) of (a) GCN and (b) D_{N_2} . The isosurface value is set to $0.03 \text{ e}/\text{\AA}^3$.

3. CO₂ ADSORPTION SIMULATION DETAILS

In this study, nine CO₂ adsorption sites were considered in both parallel and vertical orientations, which were the four atom sites, three bond sites and two interstitial sites. For clarity, the four atom sites were N1, N2, C1 and C2 sites; three bond sites being the intermediate point between C1–N2, N2–C2 and N1–C1 bonds, represented as B1, B2 and B3; lastly, the center of a triazine ring as one interstitial site (I1) and the cavity within the six-fold heptazine ring as another interstitial site (I2). The CO₂ adsorption configurations were illustrated as fixed g-C₃N₄ atoms in Figs. S3–6 to accurately portray the position of the CO₂ molecule on these structures. Optimization of separation distance between CO₂ molecule and g-C₃N₄ surface was performed, and the ideal distance was discovered to be at 2.5 Å.

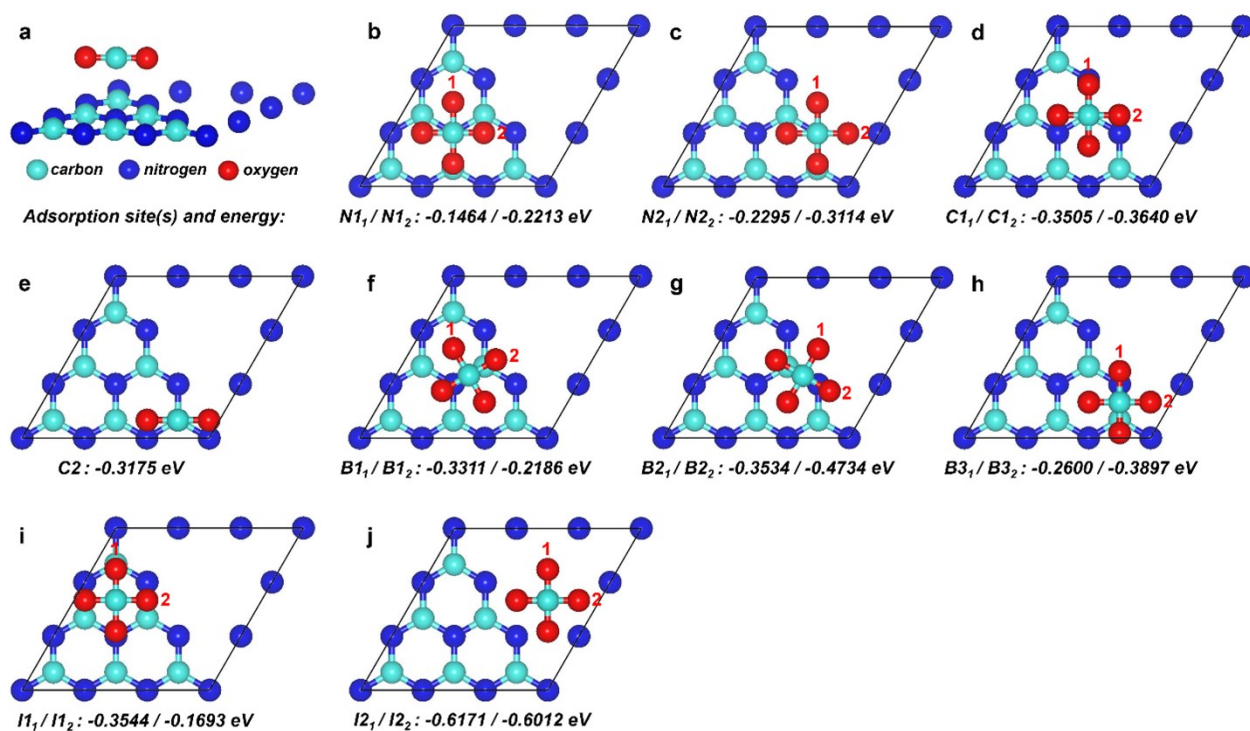


Fig. S3 (a) Side view of CO₂ molecule adsorbed on GCN in parallel orientation. (b-j) Top view of CO₂ molecule adsorbed on GCN in parallel orientation at different adsorption sites with their corresponding adsorption energy, E_{ads} . The number denotes the rotation angle of CO₂ molecule at various points.

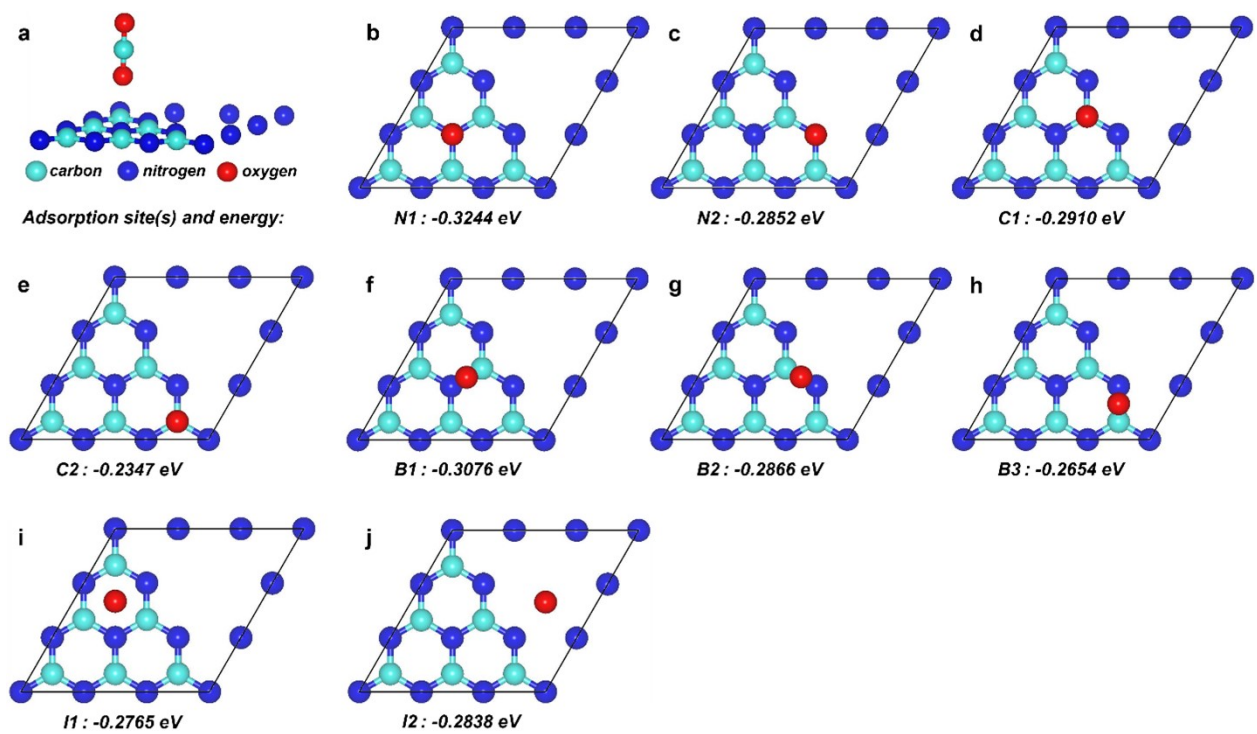


Fig. S4 (a) Side view of CO₂ molecule adsorbed on GCN in vertical orientation. (b-j) Top view of CO₂ molecule adsorbed on GCN in vertical orientation at different adsorption sites with their corresponding adsorption energy, E_{ads} .

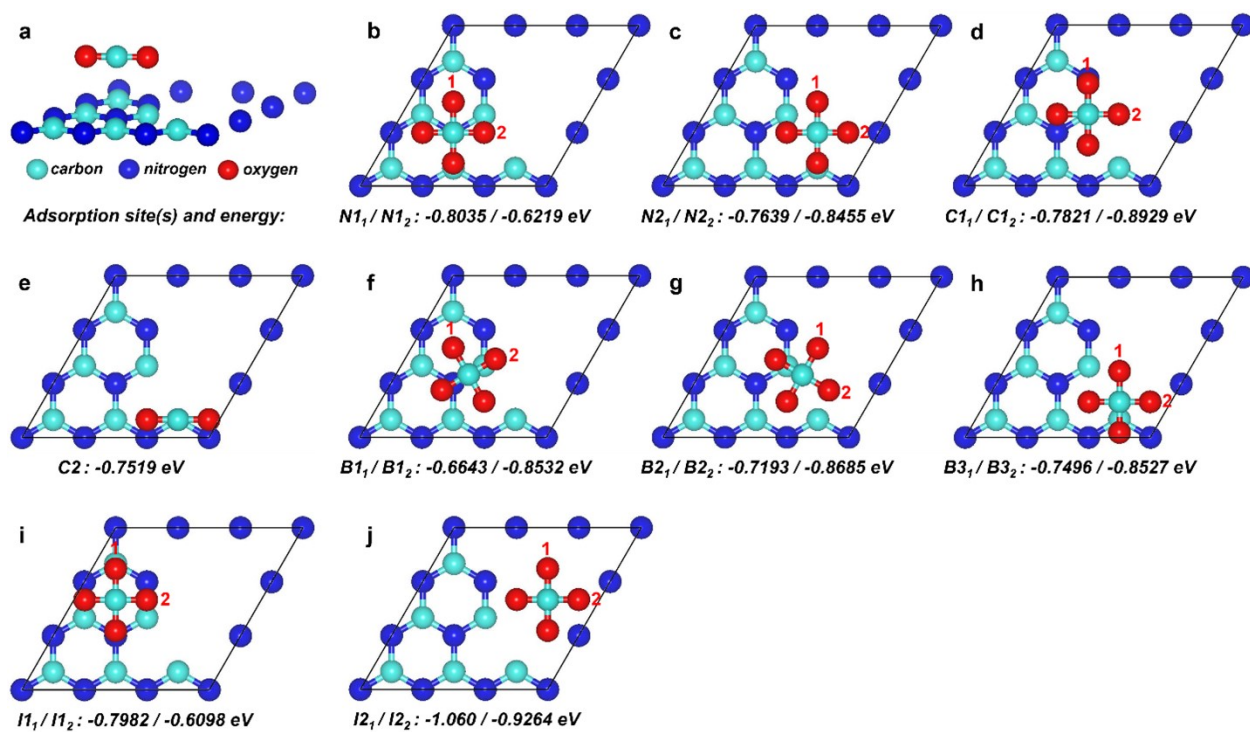


Fig. S5 (a) Side view of CO₂ molecule adsorbed on D_{N2} in parallel orientation. (b-j) Top view of CO₂ molecule adsorbed on D_{N2} in parallel orientation at different adsorption sites with their corresponding adsorption energy, E_{ads} . The number denotes the rotation angle of CO₂ molecule at various points.

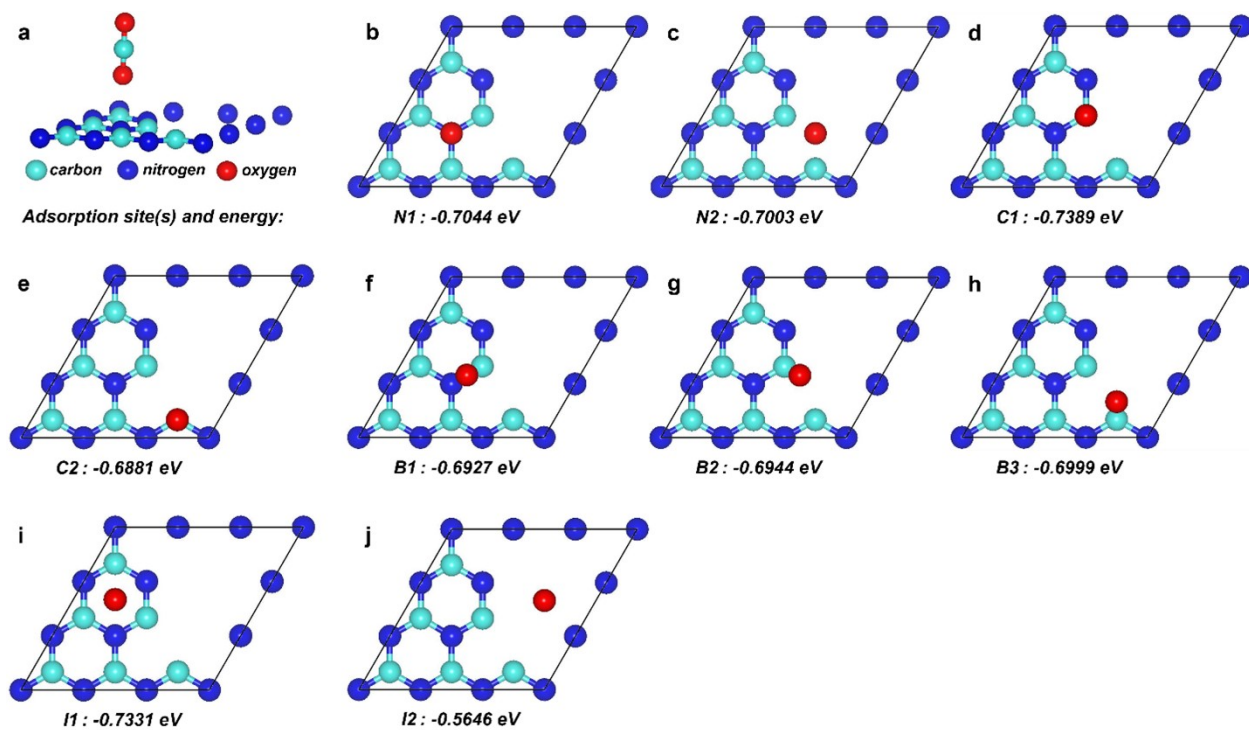


Fig. S6 (a) Side view of CO_2 molecule adsorbed on D_{N_2} in vertical orientation. (b-j) Top view of CO_2 molecule adsorbed on D_{N_2} in vertical orientation at different adsorption sites with their corresponding adsorption energy, E_{ads} .

4. GIBBS FREE ENERGY CHANGE

Table S1 The calculated change in Gibbs free energy of all elementary steps for CO₂ reduction pathways on GCN and D_{N2}.

CO Formation								
Elementary Steps	GCN				D _{N2}			
	ΔE	ΔE_{ZPE}	$T\Delta S$	ΔG	ΔE	ΔE_{ZPE}	$T\Delta S$	ΔG
*+ CO ₂	0.00	0.00	0.00	0.00	0.00	0.00	0.00	0.00
CO ₂ * + H ⁺ + e ⁻	0.32	0.01	0.33	0.64	-0.44	0.01	0.33	-0.12
TS _{HCOO} *	2.11	0.26	0.51	2.36	1.53	0.26	0.51	1.78
HCOO*	1.64	0.00	0.11	1.74	1.07	0.00	0.11	1.17
TS _(CO* + OH*)	3.73	0.18	0.31	3.86	2.20	0.18	0.31	2.33
CO* + OH*	3.29	0.11	0.19	3.37	1.75	0.11	0.19	1.83
CO + OH* + H ⁺ + e ⁻	0.46	0.05	0.30	0.71	-1.22	0.05	0.30	-0.97
TS _(CO + H₂O*)	3.27	0.07	0.52	3.72	1.17	0.07	0.52	1.62
CO + H ₂ O*	0.90	0.29	0.20	0.81	-0.52	0.29	0.20	-0.61
CO + H ₂ O + *	0.79	0.19	0.24	0.84	-0.98	0.19	0.24	-0.93
CH ₃ OH Formation								
Elementary Steps	GCN				D _{N2}			
	ΔE	ΔE_{ZPE}	$T\Delta S$	ΔG	ΔE	ΔE_{ZPE}	$T\Delta S$	ΔG
*+ CO ₂	0.00	0.00	0.00	0.00	0.00	0.00	0.00	0.00
CO ₂ * + H ⁺ + e ⁻	0.96	0.01	0.33	0.64	0.20	0.01	0.33	-0.12
TS _{HCOO} *	2.61	0.26	0.51	2.36	2.03	0.26	0.51	1.78
HCOO*	1.84	0.00	0.11	1.74	1.27	0.00	0.11	1.17
HCOO* + H ⁺ + e ⁻	1.98	0.22	0.09	2.11	0.49	0.22	0.09	0.62
TS _{HCOOH} *	1.88	0.61	0.24	2.25	2.53	0.61	0.24	2.90
HCOOH*	1.86	0.06	0.57	1.35	-0.21	0.06	0.57	-0.72
HCOOH* + H ⁺ + e ⁻	0.93	0.11	0.21	0.84	-0.34	0.11	0.21	-0.43
TS _(HCO* + H₂O*)	2.55	0.30	0.68	2.17	2.68	0.30	0.68	2.30
HCO* + H ₂ O*	1.63	0.21	0.54	1.30	0.81	0.21	0.54	0.48
HCO* + H ₂ O* + H ⁺ + e ⁻	1.95	0.02	0.77	1.20	1.17	0.02	0.77	0.42
TS _{(CH₂O*) + H₂O*}	2.47	0.01	0.40	2.08	2.35	0.01	0.40	1.96
CH ₂ O* + H ₂ O*	2.14	0.25	0.28	2.11	1.61	0.25	0.28	1.58

$CH_2O^* + H_2O^* + H^+ + e^-$	2.23	0.24	0.54	1.93	1.34	0.24	0.54	1.04
$TS_-(CH_2OH^*) + H_2O^*$	2.97	0.23	0.23	2.97	3.40	0.23	0.23	3.40
$CH_2OH^* + H_2O^*$	1.03	0.04	0.38	0.70	0.11	0.04	0.38	-0.22
$CH_2OH^* + H_2O^* + H^+ + e^-$	1.03	0.14	0.31	0.86	-0.80	0.14	0.31	-0.97
$TS_-(CH_3OH^*) + H_2O^*$	1.88	0.65	0.48	2.05	0.00	0.65	0.48	0.17
$CH_3OH^* + H_2O^*$	0.62	0.29	0.60	0.31	-0.49	0.29	0.60	-0.80
$CH_3OH^* + H_2O$	0.04	0.03	0.34	-0.27	-1.30	0.03	0.34	-1.61
$CH_3OH + H_2O + *$	-0.18	0.06	0.18	-0.30	-2.00	0.06	0.18	-2.12
CH₄ Formation								
Elementary Steps	GCN				D _{N2}			
	ΔE	ΔE_{ZPE}	$T\Delta S$	ΔG	ΔE	ΔE_{ZPE}	$T\Delta S$	ΔG
*+ CO ₂	0.00	0.00	0.00	0.00	0.00	0.00	0.00	0.00
CO ₂ * + H ⁺ + e ⁻	0.56	0.41	0.33	0.64	-0.20	0.41	0.33	-0.12
TS_HCOO*	2.61	0.26	0.51	2.36	2.03	0.26	0.51	1.78
HCOO*	1.84	0.00	0.11	1.74	1.27	0.00	0.11	1.17
HCOO* + H ⁺ + e ⁻	1.98	0.22	0.09	2.11	0.49	0.22	0.09	0.62
TS_HCOOH*	1.88	0.61	0.24	2.25	2.53	0.61	0.24	2.90
HCOOH*	1.86	0.06	0.57	1.35	-0.21	0.06	0.57	-0.72
HCOOH* + H ⁺ + e ⁻	0.93	0.11	0.21	0.84	-0.34	0.11	0.21	-0.43
TS_-(HCO* + H ₂ O*)	2.55	0.30	0.68	2.17	2.68	0.30	0.68	2.30
HCO* + H ₂ O*	1.63	0.21	0.54	1.30	0.81	0.21	0.54	0.48
HCO* + H ₂ O* + H ⁺ + e ⁻	1.95	0.02	0.77	1.20	1.17	0.02	0.77	0.42
TS_-(CH ₂ O*) + H ₂ O*	2.47	0.01	0.40	2.08	2.35	0.01	0.40	1.96
CH ₂ O* + H ₂ O*	2.14	0.25	0.28	2.11	1.61	0.25	0.28	1.58
CH ₂ O* + H ₂ O* + H ⁺ + e ⁻	2.23	0.24	0.54	1.93	1.34	0.24	0.54	1.04
TS_-(CH ₂ OH*) + H ₂ O*	2.97	0.23	0.23	2.97	3.40	0.23	0.23	3.40
CH ₂ OH* + H ₂ O*	1.03	0.04	0.38	0.70	0.11	0.04	0.38	-0.22
CH ₂ OH* + H ₂ O + H ⁺ + e ⁻	3.15	0.16	0.47	2.84	1.46	0.16	0.47	1.15
TS_-(CH ₂ * + H ₂ O*)	4.30	0.11	0.44	3.97	2.56	0.11	0.44	2.23
CH ₂ * + H ₂ O*	1.51	0.43	0.35	1.59	-0.05	0.43	0.35	0.03
CH ₂ * + H ₂ O* + H ⁺ + e ⁻	2.13	0.03	0.52	1.64	0.19	0.03	0.52	-0.30

$TS_-(CH_3^*) + H_2O^*$	2.77	0.24	0.28	2.73	0.80	0.24	0.28	0.76
$CH_3^* + H_2O^*$	0.63	0.20	0.35	0.48	-1.21	0.20	0.35	-1.36
$CH_3^* + H_2O^* + H^+ + e^-$	0.61	0.17	0.22	0.56	-1.43	0.17	0.22	-1.48
$TS_-(CH_4^*) + H_2O^*$	2.00	0.00	0.29	1.71	-0.01	0.00	0.29	-0.30
$CH_4^* + H_2O^*$	-0.85	0.30	0.19	-0.75	-2.77	0.30	0.19	-2.67
$CH_4^* + H_2O$	-0.70	0.10	0.22	-0.82	-2.74	0.10	0.22	-2.86
$CH_4 + H_2O + *$	-0.67	0.13	0.30	-0.84	-2.74	0.13	0.30	-2.91